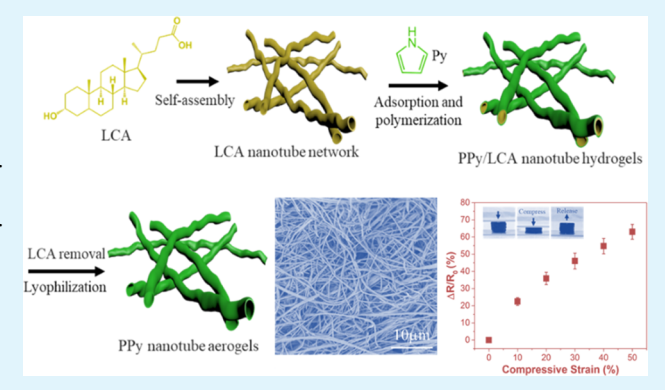


# Soft-Templated Synthesis of Lightweight, Elastic, and Conductive **Nanotube Aerogels**

Wenlang Liang,†,‡ Samuel Rhodes,‡ Jianlu Zheng,§ Xiaochen Wang,‡ and Jiyu Fang\*,‡®

Supporting Information

ABSTRACT: Conductive polymer (CP) nanotubes are fascinating nanostructures with high electrical conductivity, fast charge/discharge capability, and high mechanical strength. Despite these attractive physical properties, progress in the synthesis of CP nanotube hydrogels is still limited. Here, we report a facile and effective approach for the synthesis of polypyrrole (PPy) nanotube hydrogels by using the weakly interconnected network of self-assembled nanotubes of lithocholic acid as a soft template. The PPy nanotube hydrogels are then converted to aerogels by freeze drying, in which PPy nanotubes form elastic and conductive networks with a density of 38 mg/cm<sup>3</sup> and an electrical conductivity of 1.13 S/m. The PPy nanotube aerogels are able to sustain a compressive strain as high as 70% and show an excellent cyclic compressibility due



to their robust nanotube networks and hierarchically porous structures, which allow the compressive stress to be easily dissipated. Furthermore, PPy nanotube aerogels show negative strain-dependent electrical resistance changes under compressive strains. The lightweight, elastic, and conductive PPy nanotube aerogels may find potential applications in strain sensors, supercapacitors, and tissue scaffolds.

KEYWORDS: conductive polymers, nanotubes, hydrogels and aerogels, compressibility, electrical conductivity

## 1. INTRODUCTION

Conducting polymers (CP) have attracted great interest in both academia and industry over the past few decades. In recent years, one-dimensional CP nanostructures have emerged as one of the exciting research areas in nanoscience and nanotechnology.<sup>2-10</sup> Among them, CP nanotubes are especially interesting because they offer a unique combination of large surface area, superior electrical conductivity, excellent electrochemical activity, and good mechanical properties.<sup>2,3,7</sup> It has been reported that the electrical conductivity of CP nanotubes is in the range of 1-50 S/cm, 11-13 which is much higher than that of their globular forms  $(10^{-1}-10^{-2} \text{ S/cm})$ . The short diffusion path of CP nanotubes for ion transport leads to the rapid redox switching (<10 ms).<sup>14</sup> The large surface area of CP nanotubes allows to achieve high charge/ discharge capacities, which are critical for developing their applications in supercapacitors. 15,16 Furthermore, the elastic modulus of CP nanotubes can reach as high as 60 GPa due to the easy dissipation of stress through their hollow structures. 17,18

The large-scale assembly of CP nanotubes holds the key for their applications in devices. Recently, the ordered array of CP nanotubes has been fabricated on substrates for electrochromic displays, <sup>19</sup> solar cells, <sup>20</sup> and sensors. <sup>21,22</sup> Conducting polymer hydrogels and aerogels are a new class of materials.<sup>23</sup> Due to the high conductive network, large surface area, short diffusion path, and high electrochemical activity, conductive polymer hydrogels and aerogels have been used in energy storages, <sup>24–26</sup> artificial skins,<sup>27</sup> separations,<sup>28</sup> sensors,<sup>9–31</sup> and tissue engineering.32-34

CP nanotubes are promising candidates for designing elastic and conductive hydrogels and aerogels, in which the advantages of CP nanotubes and cross-linked networks can be synergized. However, progress in the synthesis of elastic CP nanotube hydrogels and aerogels is still limited due to the challenge of assembling them into interconnected networks over a large area.<sup>35</sup> Herein, we report a facile and effective templated synthesis of polypyrrole (PPy) nanotube hydrogels by the polymerization of the pyrrole adsorbed on the interconnected network of self-assembled lithocholic acid

Received: August 15, 2018 Accepted: October 5, 2018 Published: October 5, 2018



<sup>&</sup>lt;sup>†</sup>College of Materials Science and Engineering, Southwest Jiaotong University, Chengdu 610031, China

<sup>\*</sup>Advanced Materials Processing and Analysis Center, Department of Materials Science and Engineering, University of Central Florida, Orlando, Florida 32816, United States

<sup>&</sup>lt;sup>§</sup>College of Materials Science and Engineering, Shenzhen University, Shenzhen 518060, Sichuan, China

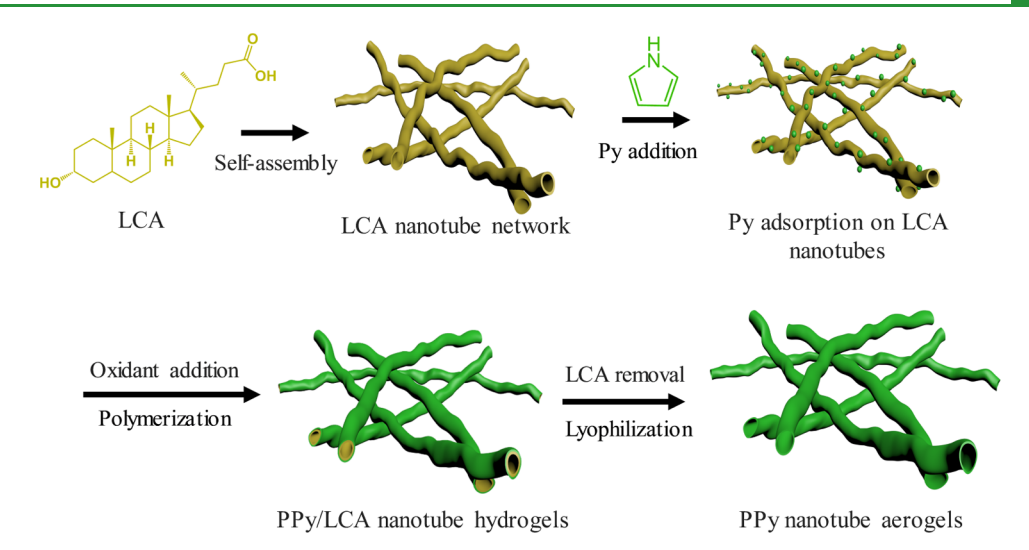


Figure 1. Schematic representation of the synthesis procedure of PPy nanotube hydrogels and aerogels by using the interconnected LCA nanotube network as a soft template.

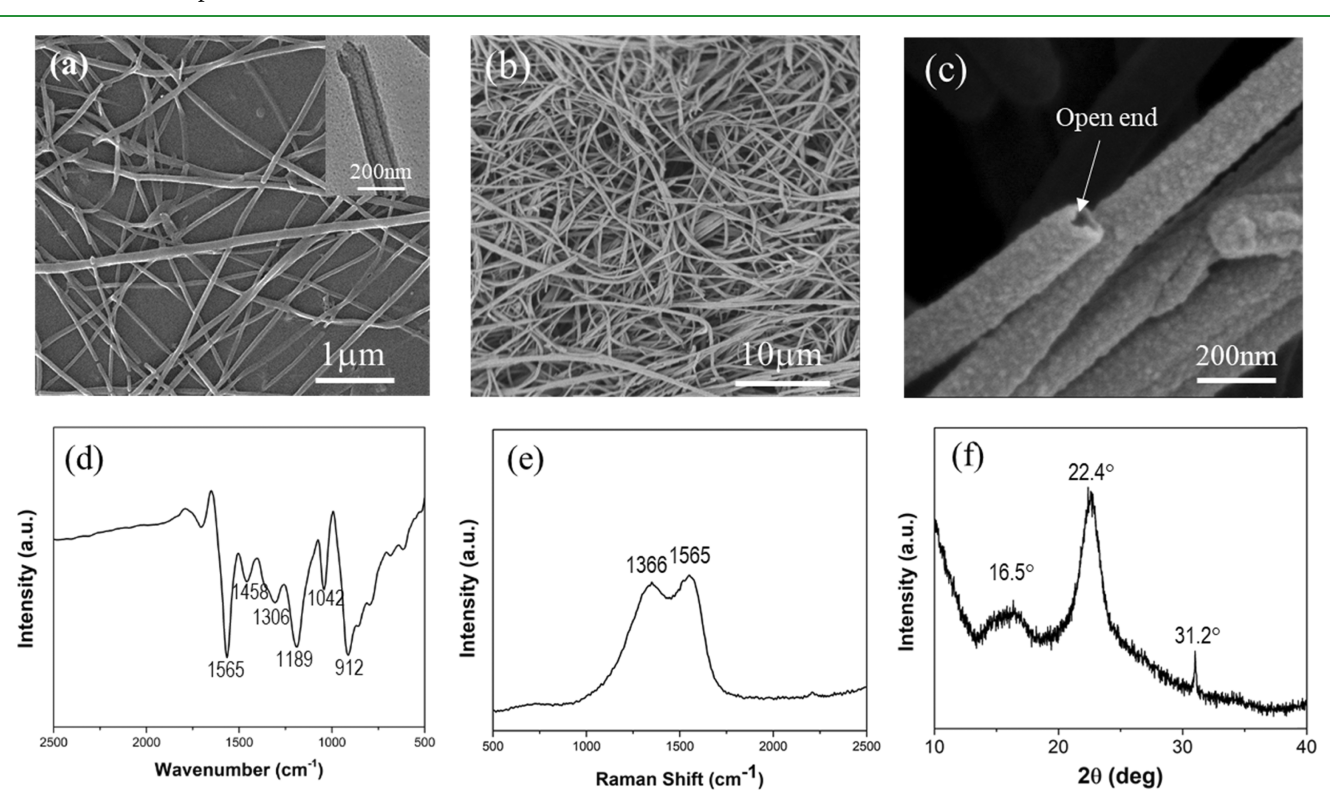


Figure 2. SEM images of self-assembled LCA nanotube networks (a) and PPy nanotube aerogels (b, c). FT-IR (d) and Raman (e) spectra of PPy nanotube aerogels. (f) X-ray diffraction of PPy nanotube aerogels. TEM image of LCA nanotubes is inserted in (a).

(LCA) nanotubes (Figure 1). The PPy nanotube hydrogels are subsequently converted to lightweight, elastic, and conductive aerogels with hierarchical porous structures by freeze drying. The unique physical properties of PPy nanotube aerogels make them excellent candidates for potential applications in strain sensors, supercapacitors, and tissue engineering.

## 2. EXPERIMENTAL SECTION

2.1. Materials. Lithocholic acid (LCA), sodium hydroxide (NaOH), sodium peroxydisulfate (SPS), and pyrrole (Py) were purchased from Sigma-Aldrich and used as received without further purification. Water used in the experiments was purified with the Easypure II system (18 M $\Omega$  cm, pH 5.7).

2.2. Formation of LCA Nanotubes. LCA was added in 1 M NaOH solution in a glass vial to achieve a final concentration of 50 mM, followed by 5 min sonication in an ultrasonic bath (Branson 1510, Branson Ultrasonics Co.) at 50 °C for 30 min. LCA solution was then cooled to room temperature.

2.3. Formation of PPy Nanotube Hydrogels and Aerogels. Pyrrole with different concentrations was added to 1 mL of LCA nanotube solution to achieve a final concentration of 72.5, 145, and 290 mM. The mixtures were incubated for 1 h for the adsorption of pyrrole on LCA nanotube networks, followed by the addition of 150, 300, and 600  $\mu L$  of 2 M SPS solution. The samples were kept in a water bath at 3 °C for 24 h. The polymerization of the pyrrole adsorbed on LCA nanotube networks proceeded without stirring. Finally, the templated PPy nanotube hydrogels were collected by

breaking the glass vial and then washed multiple times with deionized water and ethanol alternatively to remove excess ions and LCA templates. PPy nanotube aerogels were prepared by the lyophilization of PPy nanotube hydrogels with a freeze dryer (LGJ-18A, Beijing Sihuan Instrument Company, China) at -70 °C under vacuum for 24

2.4. Characterization. Transmission electron microscopy (TEM) measurements of LCA nanotubes dried on a carbon film-coated copper grid were performed on a JEOL TEM-1011 operated at 100 kV. Scanning electron microscopy (SEM) measurements of PPy nanotube hydrogels dried on a silicon wafer were carried out with a Zeiss Ultra-55 FEG SEM operated at 20 kV. Fourier transforminfrared (FT-IR) spectra were recorded with a Perkin-Elmer (100) spectrometer operating at 4 cm<sup>-1</sup> resolution. Raman scattering measurements were performed with a multichannel modular triple Raman system (Renishaw Co.). ζ-Potential measurements were carried out with a Zetasizer Nano ZS90 (Malvern Instruments Inc.) at room temperature under a cell driven voltage of 30 V. For the compressive stress-strain measurements, PPy nanotube aerogels were placed between two glass slides and compressed at 0.1 mm/s with a Micro-Force Test System (Tytron 250, MTS Systems Corp.). The rheological measurements were performed on an AR2000-EX rheometer (TA Instrument) with a cone plate geometry on a Peltier plate in the angular frequency ranging from 0.1 to 100 rad/s at room temperature. The electrical properties of PPy nanotube aerogels were measured with a sourcemeter (Keithley, model 2400) and a four-point probe method (RTS-9, Four Probe Tech. China).

### 3. RESULTS AND DISCUSSION

LCA is a naturally occurring biological surfactant.<sup>36</sup> It consists of a rigid, quasi-planar steroid backbone and a carboxylic acid group linked to the steroid backbone through a short alkyl chain (Figure 1). In alkaline aqueous solution, LCA can selfassemble into tubule structures with different diameters and shapes, depending on the condition under which the self-assembly occurs, 37-42 which can further interact with each other to form weakly interconnected networks. In our experiments, the self-assembly of LCA was carried out in 0.1 M NaOH solution. After LCA solution is aged for 2 days at room temperature, the formation of long LCA nanotubes with an average diameter of  $\sim$ 140 nm is observed (Figure 2a). The hollowness and open end of LCA nanotubes can be seen from the TEM image inserted in Figure 2a. The wall thickness of LCA nanotubes is  $\sim$ 13 nm, which is almost 8 times larger than the length of LCA measured from its OH group to the COOH group (~1.5 nm), suggesting that LCA molecules form a lamellar structure in the nanotube wall. The LCA nanotubes interconnect to form networks. However, the network is unable to hold water to form a stable hydrogel due to the weak interaction at the contact point between LCA nanotubes (Figure S1a). This result agrees with the viscoelastic measurements which showed that the weakly interconnected LCA nanotubes were unable to form a permanent network.<sup>37</sup>

We found that the weakly interconnected LCA nanotube network in NaOH solution can serve as a soft template for the synthesis of PPy nanotube hydrogels. In our experiments, pyrrole (Py) was added in 1 mL of LCA nanotube solution to achieve a final concentration of 72.5 mM. After 1 h of incubation, 150  $\mu$ L of 2 M SPS solution was added. The mixed solution turns into black hydrogels after being kept in a water bath at 3 °C for 24 h (Figure S1b). The  $pK_a$  value of LCA is ~7.0. In 0.1 M NaOH solution, the COOH group of LCA is deprotonated. 39,40 The  $\zeta$ -potential of LCA nanotubes is -31mV, suggesting that the COO- group of LCA presents at the surface of the nanotubes. The adsorption of pyrrole on LCA

nanotubes is likely due to the hydrogen bonding between the NH group of the pyrrole and the COO<sup>-</sup> group of the LCA. The formation of the hydrogen bonding between the NH group of organic amines and the COO- group of LCA was reported in the literature.<sup>38</sup> The polymerization of the pyrrole adsorbed on LCA nanotube networks by SPS oxidant leads to the formation of PPy nanotube hydrogels. The templated PPy nanotube hydrogels were collected by breaking the glass vial. They remain intact after being taken off from the broken glass vial (Figure S1c) and then washed with deionized water and ethanol alternatively for multiple times and dried at -70 °C under vacuum for 24 h. The resulting PPy nanotube aerogels slightly shrink in their volumes, compared to PPy nanotube hydrogels, but show a significant weight loss (96%). The density of PPy nanotube aerogels is measured to be ~38 mg/ cm<sup>3</sup>. The morphology of PPy nanotube aerogels was investigated with SEM, which clearly shows the interconnected network of PPy nanotubes with the pore size of a few microns (Figure 2b). The PPy nanotubes have an average diameter of  $\sim$ 170 nm with a rough surface (Figure 2c). The hollowness of the PPy nanotubes is evident from their open ends marked with an arrow in Figure 2c. The internal diameter of the PPy nanotube measured from the open end is ~130 nm, which is close to the average diameter of LCA nanotubes. The hollowness of the PPy nanotubes suggests that the adsorption of PPy occurs on the surface of LCA nanotubes rather than inside the cavity of LCA nanotubes. It was reported that the polarity of water confined in organic nanotubes is lower than that of bulk water 43 and the diffusion of molecules in water confined in organic nanotubes is slower than that in bulk water.44 This may explain why the adsorption of PPy does not occur inside the cavity of the LCA nanotube. The PPy nanotube aerogels have hierarchical porous structures. The Fourier transform-infrared (FT-IR) spectrum of PPy nanotube aerogels shows several characteristic vibrations of PPy (Figure 2d). The peaks at 1565 and 1458 cm<sup>-1</sup> are attributed to the fundamental vibrations of the polypyrrole ring. The peaks at 1306, 1189, 1042, and 912 cm<sup>-1</sup> can be assigned to the C-N stretching in the ring, the C-H in plane deformation vibration, the N-H in plane deformation vibration, and the C-H out-ofplane ring deformation vibration, respectively. 45,46 The stretching vibration of the COO- group of LCA at 1626 cm<sup>-1</sup> is not observed, suggesting the removal of LCA nanotube templates by the washing process. The Raman spectrum of PPy nanotube aerogels shows two bands at 1565 and 1366 cm<sup>-1</sup> (Figure 2e), which are corresponding to the C=C stretching vibration and C-C stretching vibration of the pyrrole ring, respectively.<sup>47</sup> These characteristic FT-IR and Raman peaks confirm the successful polymerization of pyrrole on the surface of LCA nanotube networks. PPy nanotubes show three X-ray diffraction peaks, suggesting that they have a crystalline structure (Figure 2f). The broad peak centered at  $2\theta = 16.5^{\circ}$ (d = 5.37 Å) and the sharp peak at  $2\theta = 22.4^{\circ}$  (d = 3.97 Å)may be ascribed to the periodicities, which are parallel and perpendicular to PPy chains, respectively. 48,49

In the templated synthesis, the polymerization of pyrrole may start either in the aqueous solution confined in LCA nanotube networks or on the surface of LCA nanotubes, depending on the location of pyrrole in the network. The result shown in Figure 2b indicates that the surface polymerization is overwhelmed due to the adsorption of pyrrole on LCA nanotubes. However, if excess pyrrole presents in the aqueous solution confined within the LCA nanotube network, the

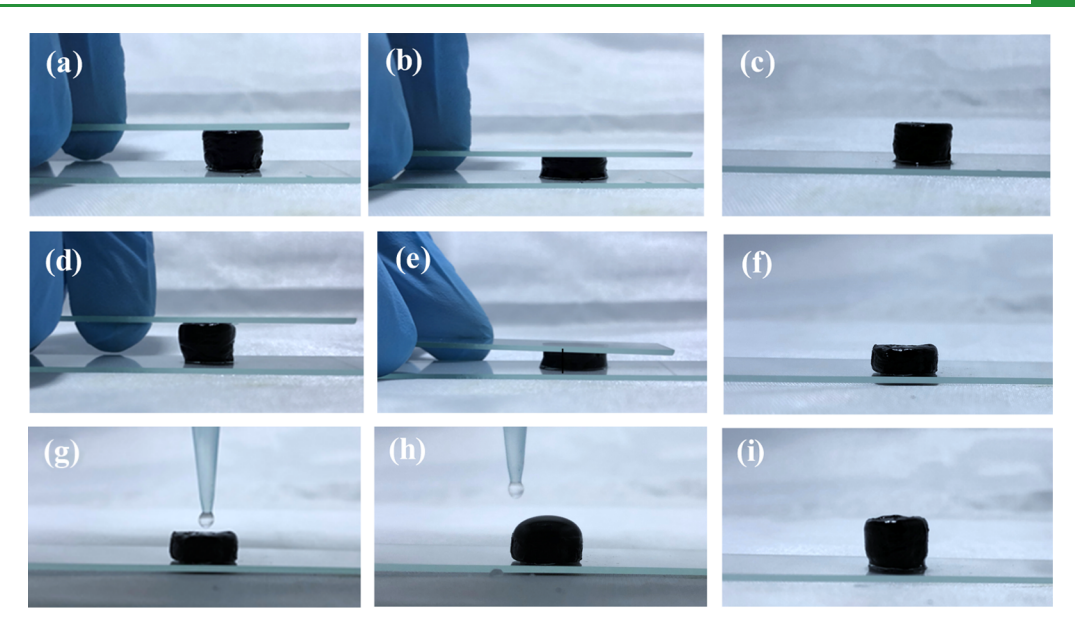


Figure 3. Photographic images of the compression and recovery of PPy nanotube hydrogels. (a, b) The compression of PPy nanotube aerogels to ~50%. (c) The recovery of PPy nanotube aerogels from ~50% compression after the removal of loading. (d, e) The compression of PPy nanotube aerogels to ~70%. (f) The recovery of PPy nanotube aerogels from ~70% compression after the removal of loading. (g, h, i) The recovery of compressed PPy nanotube aerogels by absorbing water.

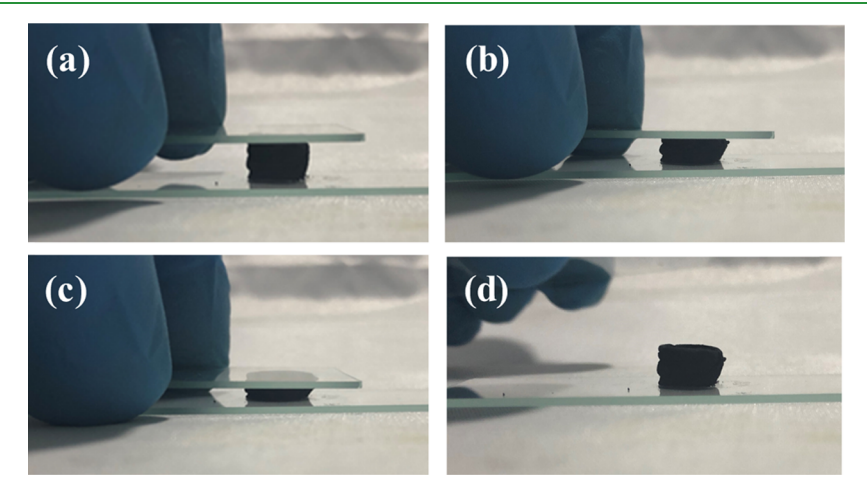


Figure 4. Photographic images of the compression of PPy nanotube aerogels to ~70% (a-c) and the recovery of PPy nanotube aerogels from  $\sim$ 70% compression after the removal of loading (d).

solution polymerization occurs as well. For the efficient oxidation of Py, the ratio of Py and SPS was always kept at near 1:2 in our experiments. PPy nanotube aerogels were formed by the addition of 145 and 290 mM pyrrole into 1 mL LCA nanotube solution, followed by the addition of 300 and 600 µL of 2 M SPS solution, respectively. In both cases, the formation of PPy granules on PPy nanotubes and within PPy nanotube networks is clearly observed (Figure S2). The control experiments showed that PPy prepared in NaOH aqueous solution without LCA nanotubes was in the form of granules (Figure S3). The number of PPy granules within PPy nanotube networks increases with the increase of pyrrole concentrations. The PPy nanotube aerogels with a large amount of PPy granules suffer from structural fatigue. They easily break apart under repeated compression because the presence of a large amount of PPy granules prevents the effective crosslinks of PPy nanotube networks.

PPy nanotube hydrogels formed at the Py concentration of 72.5 mM are able to sustain a large compressive strain without

structural fracture. For example, the PPy nanotube hydrogel cylinder compressed by ~50% recovers to its original height after the removal of the compressive loading (Figure 3a-c). However, if the PPy nanotube hydrogel cylinder is compressed by ~70%, it is unable to fully recover its original height when the loading is removed (Figure 3d-f). Under the large compressive strain, the PPy nanotubes may buckle or come together in the network, leading to the formation of new contacting points between PPy nanotubes. The hydrogen bonding of water molecules with the NH groups of PPy nanotubes at the new contacting points locks the deformation. The full recovery of the deformed PPy nanotube hydrogel cylinder can be achieved by swelling the water drops added on the top of it (Figure 3g-i), in which the swelling causes the rapid expansion of the nanotube network, breaking the hydrogen bonding at the new contacting points. PPy nanotube aerogel cylinders show excellent elasticity and fully recover to their original height from ~70% compression in a few seconds after the removal of the compressive loading (Figure 4). The

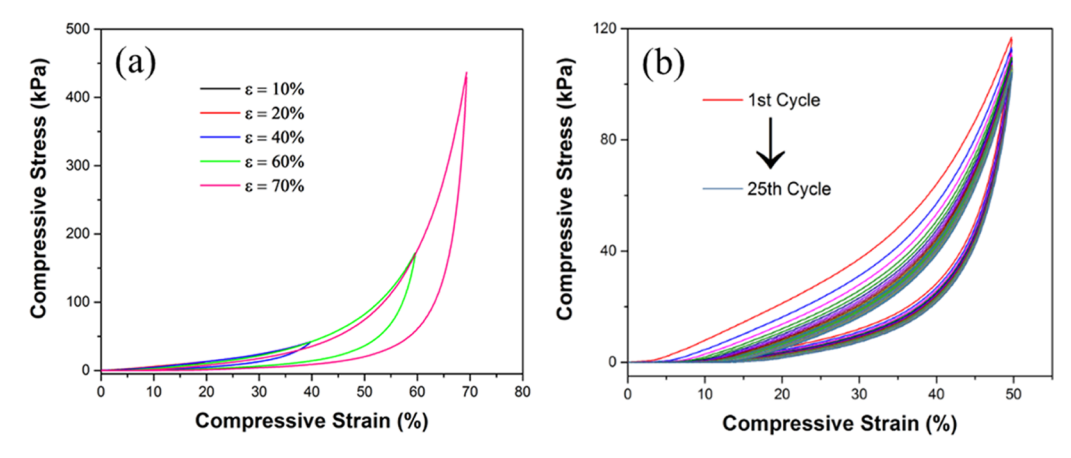


Figure 5. (a) Compressive stress ( $\sigma$ )-strain ( $\varepsilon$ ) curves of PPy nanotube aerogels at the set strain ( $\varepsilon$ ) of 10, 20, 40, 60, and 70%. (b) Cyclic stressstrain curves of PPy nanotube aerogels at  $\varepsilon = 50\%$ .

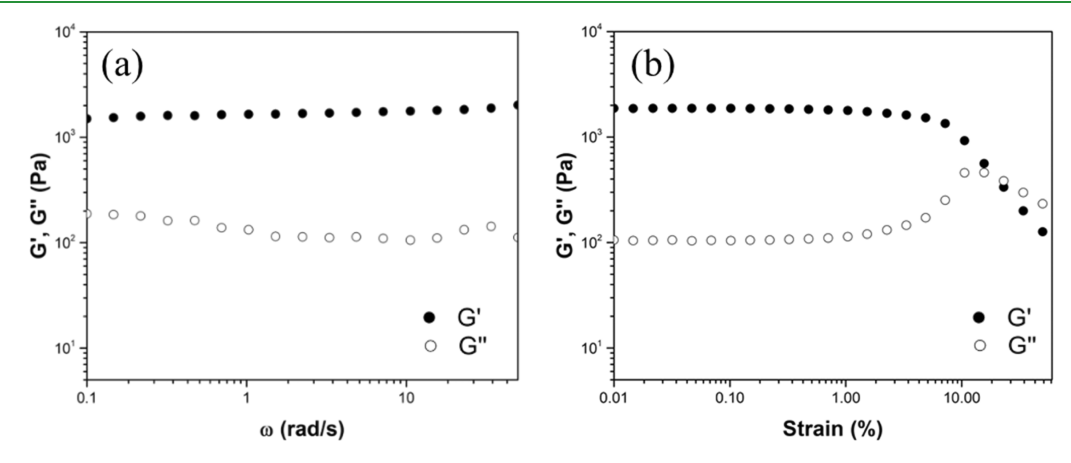


Figure 6. (a) Frequency and (b) strain sweeps of PPy nanotube aerogels at room temperature.

excellent elasticity of PPy nanotube aerogels is likely due to their hierarchical porous structures (microsized pores within the nanotube networks and nanosized holes within nanotubes), which allows the compressive stress to be easily dissipated.

To quantitatively examine the mechanical properties of PPy nanotube aerogels, especially the recyclable compressibility, a set of compressive tests was conducted under different conditions. Figure 5a shows the compressive stress  $(\sigma)$ -strain  $(\varepsilon)$  curves of PPy nanotube aerogels for the loadingunloading cycle at a series of set  $\varepsilon$  from 10 to 70%. The  $\sigma$ – $\varepsilon$  curves during the loading process are linear for  $\varepsilon$  < 20% with an elastic modulus of  $\sim$ 0.7 kPa. For  $\varepsilon$  > 20%, the  $\sigma$ - $\varepsilon$ curves become nonlinear with a rapid increasing slope. A hysteresis loop as the index of energy dissipation appears in the loading—unloading curves at  $\varepsilon = 40\%$  and expands with the increase of  $\varepsilon$ . Despite the presence of hysteresis loops, the  $\sigma$ always returns to the original value after the unloading for each  $\varepsilon$ , indicating that the PPy nanotube aerogel fully recover their original shape without plastic deformation. Figure 5b shows the  $\sigma$ - $\varepsilon$  curves of PPy nanotube aerogels during the multiple loading-unloading cycles at the set  $\varepsilon$  of 50%. After 25 loading-unloading cycles, the  $\sigma$  still recovers well without significant plastic deformation.

The PPy nanotube aerogels are further characterized by rheological measurements. Frequency sweep measurements at the fixed shear strain of 0.1% show that the storage modulus (G') and loss modulus (G'') of PPy nanotube aerogels are

slightly frequency dependent in the range of angular frequencies from 0.1 to 50 rad/s (Figure 6a), suggesting that the viscoelastic relaxation of the nanotube network is dominant. Also, the G' is almost 1 order of magnitude larger than G'', which is an indicator of a strong aerogel. The G' (10<sup>3</sup>) Pa) of PPy nanotube aerogels is of the same order of magnitude as the G' of cross-linked biopolymer gels including actin and agarose, and lysozyme. 50 The excellent storage modulus of PPy nanotube aerogels can be attributed to their hierarchical porous structures, which facilitate the storing of energy, increasing the storage modulus. Strain sweep measurements were performed on PPy nanotube aerogels from 0.1 to 100% strain at a frequency of 10 rad/s. The PPy nanotube aerogels show a linear viscoelastic region up to  $\sim$ 10% of shear strain (Figure 6b). This confirms that the frequency sweep measurement at 0.1% strain was performed within the viscoelastic region. Above 10% strain, G' starts to decrease and G'' increases due to the breakdown of PPy nanotube networks.

In addition to high elasticity, PPy nanotube aerogels show excellent electrical properties. The electrical conductivity of PPy nanotube aerogels measured with a standard four-pointprobe method is approximately 1.13 S/m at room temperature, even the PPy nanotubes have loosely packed structures in the aerogels. The excellent electrical properties of the PPy nanotube aerogels is likely due to the high conductivity of PPy nanotubes, which are known to be highly efficient for electron transports. 51,52 Furthermore, we studied the electrical

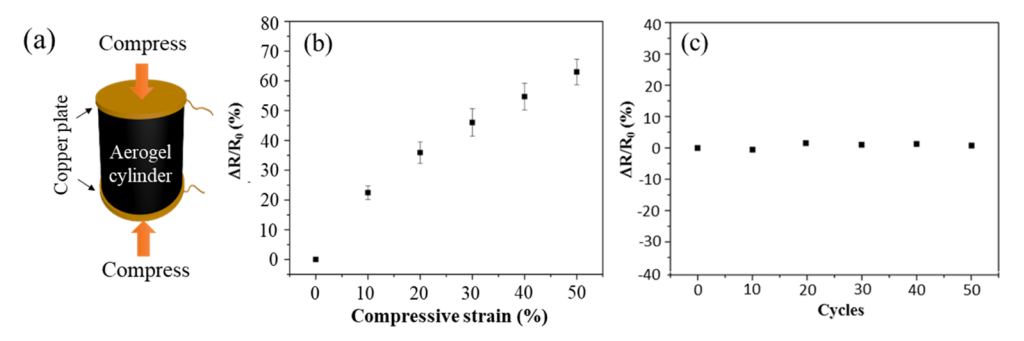


Figure 7. (a) Schematic illustration of a PPy nanotube aerogel cylinder sandwiched between two copper plate electrodes. Plot of resistance changes  $(\Delta R/R_0)$  as a function of compression strains (b) and compressive-recover cycles (c) at  $\varepsilon = 50\%$ .

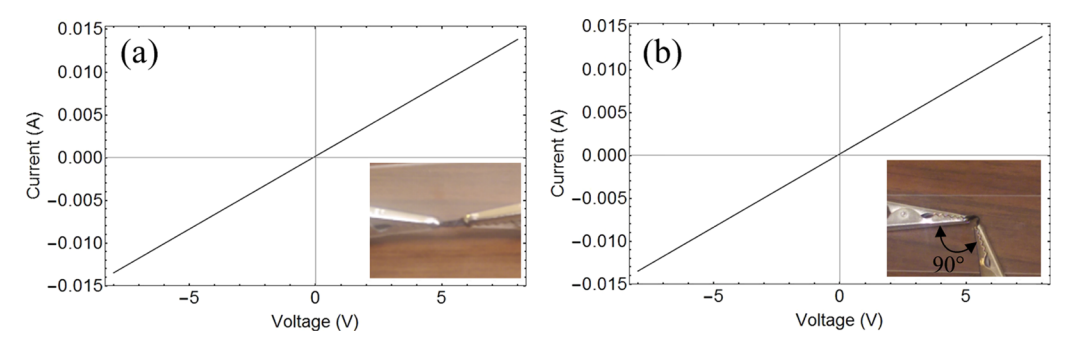


Figure 8. I (current)-V (voltage) curves of a straight (a) and bent (b) PPy aerogel sheet. Photographical images of the straight and bent PPy aerogel sheet connected in a circuit are inserted in (a) and (b), respectively.

response of PPy nanotube aerogels under compression strains, in which a PPy nanotube aerogel cylinder was sandwiched between two parallel copper plate electrodes (Figure 7a). The electrical resistance of the sandwiched PPy nanotube aerogel cylinder under compression strains was measured. To compare the relationship between electrical resistances versus compression strains, the resistance change  $(\Delta R/R_0)$  of the PPy nanotube aerogel cylinder is plotted against compressive strains, where  $\Delta R = R_0 - R$ ,  $R_0$ , and R is the resistance without and with compressive strains, respectively. As can be seen in Figure 7b,  $\Delta R/R_0$  linearly increases with the compressive strain from 0 to 50%. This result indicates that the electrical resistance of PPy nanotube aerogel cylinders decreases with the increase of compressive strains, e.g., a negative strain-dependent resistance behavior. The electrical resistance decrease of PPy nanotube aerogels under the compression is likely due to the formation of new contacting points of PPy nanotubes. Thus, the increase of the total number of conduction paths facilitates electron transfer in the network. When the loading is removed, the electrical resistance of the PPy nanotube aerogels returns to the original value because their deformation fully recovers and the newly-built contacts no longer exist. As can be seen in Figure 7c, the resistance change  $(\Delta R/R_0)$  is highly stable after multiple compression loading-unloading cycles, suggesting that the conductive network of PPy nanotubes is robust during the multiple compressions.

The PPy nanotube aerogels can be cut into small sheets (25 mm length  $\times$  0.7 mm width  $\times$  0.18 mm thickness, see the inset in Figure 8a). The current (I)-voltage (V) curve of the PPy nanotube aerogel sheet is linear (Figure 8a). The elasticity of the PPy nanotube hydrogel sheet is evident in bending tests. We find that it can be bent to an angle as large as 90° (see the inset in Figure 8b). There is no apparent change in the I-V

curve observed after the PPy nanotube hydrogel sheet is bent by 90° (Figure 8b). This result suggests that the internal conductive path of the PPy nanotube hydrogel sheet is preserved despite the large angle bending.

## 4. CONCLUSIONS

We report a facile and effective approach for the synthesis of lightweight, elastic, conductive aerogels by using the weakly interconnected network of self-assembled LCA nanotubes as a soft template, followed by a simple freeze drying process. Compared to conventional CP aerogels made of polymer chain networks, the PPy nanotube aerogels with the density of 38 mg/cm<sup>3</sup> consist of conductive nanotube networks with hierarchically porous structures, which offer them excellent mechanical and electrical properties. Despite the loosely packed PPy nanotube networks, the PPy nanotube aerogels show the electrical conductivity of 1.13 S/m, which is higher than that of many templated conductive polymer gels. They are able to sustain a compressive strain as high as 70% and show an excellent recyclable compressibility due to the robust nanotube network and the high elasticity of PPy nanotubes. Furthermore, they show negative strain-dependent electrical resistance changes. The resistance response of PPy nanotube aerogels is highly constant to the multiple compressive loading-unloading cycles. The elastic PPy nanotube hydrogels can also be cut into thin sheets, which can be bent to an angle as large as 90° without disrupting their internal conductive path. The lightweight, elastic, and conductive PPy nanotube aerogels have potential in developing strain sensors, supercapacitors, and tissue scaffolds.

#### ASSOCIATED CONTENT

## **S** Supporting Information

The Supporting Information is available free of charge on the ACS Publications website at DOI: 10.1021/acsami.8b14071.

LCA nanotube solution and PPy nanotube cylinders; SEM images of PPy nanotube aerogels and PPy granules (PDF)

#### AUTHOR INFORMATION

## **Corresponding Author**

\*E-mail: Jiyu.fang@ucf.edu.

ORCID ®

Jiyu Fang: 0000-0002-6056-5113

**Notes** 

The authors declare no competing financial interest.

#### ACKNOWLEDGMENTS

This work was supported by the U.S. National Science Foundation (CBET 1803690).

### REFERENCES

- (1) Heeger, A. J. Semiconducting and Metallic Polymers: The Fourth Generation of Polymeric Materials. Angew. Chem., Int. Ed. 2001, 40, 2591-2611.
- (2) Martin, C. R. Template Synthesis of Electronically Conductive Polymer Nanostructures. Acc. Chem. Res. 1995, 28, 61-68.
- (3) Aleshin, A. N. Polymer Nanofibers and Nanotubes: Charge Transport and Device Applications. Adv. Mater. 2006, 18, 17-27.
- (4) Wan, M. X. A Template-free Method Towards Conducting Polymer Nanostructures. Adv. Mater. 2008, 20, 2926-2932.
- (5) Tran, H. D.; Li, D.; Kaner, R. B. One Dimensional Conducting Polymer Nanostructures: Bulk Synthesis and Applications. Adv. Mater. 2009, 21, 1487-1499.
- (6) Yoon, H.; Jang, J. Conducting-Polymer Nanomaterials for High-Performance Sensor Applications: Issues and Challenges. Adv. Funct. Mater. 2009, 19, 1567-1576.
- (7) Long, Y.-Z.; Li, M.-M.; Gu, C.; Wan, M.; Duvail, J.-L.; Liu, Z.; Fan, Z. Recent Advances in Synthesis, Physical Properties and Applications of Conducting Polymer Nanotubes and Nanofibers. Prog. Polym. Sci. 2011, 36, 1415-1442.
- (8) Kim, F. S.; Ren, G.; Jenekhe, S. A. One-dimensional Nanostructures of  $\pi$ -conjugated Molecular Systems: Assembly, Properties, and Applications from Photovoltaics, Sensors, and Nanophotonics to Nanoelectronics. Chem. Mater. 2011, 23, 682-732.
- (9) Yin, Z.; Zheng, Q. Controlled Synthesis and Energy Applications of One-Dimensional Conducting Polymer Nanostructures: An Overview. Adv. Energy Mater. 2012, 2, 179-218.
- (10) Ghosh, S.; Maiyalagan, T.; Basu, R. N. Nanostructured Conducting Polymers for Energy applications: towards a sustainable platform. Nanoscale 2016, 8, 6921-6947.
- (11) Parthasarathy, R. V.; Martin, C. R. Template-Synthesized Polyaniline Microtubules. Chem. Mater. 1994, 6, 1627-1632.
- (12) Park, J. G.; Lee, S. H.; Kim, B.; Park, Y. W. Electrical Resistivity of Polypyrrole Nanotubes Measured by Conductive Scanning Probe Microscope: The Role of Contract Force. Appl. Phys. Lett. 2002, 81, 4625-4627.
- (13) Long, Y. Z.; Chen, Z. J.; Wang, N. L.; Ma, Y. J.; Zhang, Z.; Zhang, L. J.; Wan, M. W. Electrical Conductivity of a Single Conducting Polyaniline Nanotube. Appl. Phys. Lett. 2003, 83, 1863-
- (14) Cho, S. I.; Lee, S. B. Fast Electrochemistry of Conductive Polymer Nanotubes: Synthesis, Mechanism, and Application. Acc. Chem. Res. 2008, 41, 699-707.

- (15) Aricò, A. S.; Bruce, P.; Scrosati, B.; Tarascon, J.-M.; van Schalkwijk, W. Nanostructured Materials for Advanced Energy Conversion and Storage Devices. Nat. Mater. 2005, 4, 366-377.
- (16) Long, J. W.; Dunn, B.; Rolison, D. R.; White, H. S. Three-Dimensional Battery Architectures. Chem. Rev. 2004, 104, 4463-
- (17) Cuenot, S.; Demoustier-Champagne, S.; Nysten, B. Elastic Modulus of Polypyrrole Nanotubes. Phys. Rev. Lett. 2000, 85, 1690-
- (18) Cuenot, S.; Fretigny, S. C.; Demoustier-Champagne, S.; Nysten, B. Measurement of Elastic Modulus of Nanotubes with Resonant Contact Atomic Force Microscopy. J. Appl. Phys. 2003, 93, 5650-5655.
- (19) Cho, S. I.; Kwon, W. J.; Choi, S. J.; Kim, P.; Park, S. A.; Kim, J.; Son, S. J.; Xiao, R.; Kim, S. H.; Lee, S. B. Nanotube-Based Ultrafast Electrochromic Display. Adv. Mater. 2005, 17, 171-175.
- (20) Peng, T.; Sun, W.; Huang, C.; Yu, W.; Sebo, B.; Dai, Z.; Guo, S.; Zhao, X.-Z. Self-Assembled Free-Standing Polypyrrole Nanotube Membrane as an Efficient FTO- and Pt-Free Counter Electrode for Dye-Sensitized Solar Cells. ACS Appl. Mater. Interfaces 2014, 6, 14-
- (21) Kwon, O. S.; Park, S. J.; Lee, J. S.; Park, E.; Kim, T.; Park, H.-W.; You, S. A.; Yoon, H.; Jang, J. Multidimensional Conducting Polymer Nanotubes for Ultrasensitive Chemical Nerve Agent Sensing. Nano Lett. 2012, 12, 2797-2802.
- (22) Xue, M.; Li, F. W.; Chen, D.; Yang, Z. H.; Wang, X. W.; Ji, J. H. High-Oriented Polypyrrole Nanotubes for Next-Generation Gas Sensor. Adv. Mater. 2016, 28, 8265-8270.
- (23) Zhao, F.; Shi, Y.; Pan, L.; Yu, G. Multifunctional Nanostructured Conductive Polymer Gels: Synthesis, Properties, and Applications. Acc. Chem. Res. 2017, 50, 1734-1743.
- (24) Pan, L.; Yu, G.; Zhai, D.; Lee, H. R.; Zhao, W.; Liu, N.; Wang, H.; Tee, B. C.-K.; Shi, Y.; Cui, Y.; Bao, Z. Hierarchical Nanostructured Conducting Polymer Hydrogels with High Electrochemical Activity. Proc. Natl. Acad. Sci. U.S.A. 2012, 109, 9287-9292.
- (25) Hao, G.-P.; Hippauf, F.; Oschatz, M.; Wisser, F. M.; Leifert, A.; Nickel, W.; Mohamed-Noriega, N.; Zheng, Z.; Kaskel, S. Stretchable and Semitransparent Conductive Hybrid Hydrogels for Flexible Supercapacitors. ACS Nano 2014, 8, 7138-7146.
- (26) Shi, Y.; Pan, L.; Liu, B.; Wang, Y.; Cui, Y.; Bao, Z.; Yu, G. Nanostructured Conductive Polypyrrole Hydrogels as High-Performance, Flexible Supercapacitor Electrodes. J. Mater. Chem. A. 2014, 2, 6086-6091.
- (27) Hur, J.; Im, K.; Kim, S. W.; Kim, J.; Chung, D.-Y.; Kim, T.-H.; Jo, K. H.; Hahn, J. H.; Bao, Z.; Hwang, S.; Park, N. Polypyrrole/ Agarose-Based Electronically Conductive and Reversibly Restorable Hydrogel. ACS Nano 2014, 8, 10066-10076.
- (28) Lu, Y.; He, W.; Cao, T.; Guo, H.; Zhang, Y.; Li, Q.; Shao, Z.; Cui, Y.; Zhang, X. Elastic, Conductive, Polymeric Hydrogels and Sponges. Sci. Rep. 2014, 4, No. 5792.
- (29) Zhai, D.; Liu, B.; Shi, Y.; Pan, L.; Wang, Y.; Li, W.; Zhang, R.; Yu, G. Highly Sensitive Glucose Sensor Based on Pt Nanoparticle/ Polyaniline Hydrogel Heterostructures. ACS Nano 2013, 7, 3540-
- (30) Li, L.; Wang, Y.; Pan, L.; Shi, Y.; Cheng, W.; Shi, Y.; Yu, G. Nanostructured Conductive Hydrogels-Based Biosensor Platform for Human Metabolite Detection. Nano Lett. 2015, 15, 1146-1151.
- (31) He, W.; Li, G.; Zhang, S.; Wei, Y.; Wang, J.; Li, Q.; Zhang, X. Polypyrrole/Silver Coaxial Nanowire Aero-Sponges for Temperature-Independent Stress Sensing and Stress-Triggered Joule Heating. ACS Nano 2015, 9, 4244-4251.
- (32) Mawad, D.; Stewart, E.; Officer, D. L.; Romeo, T.; Wagner, P.; Wagner, K.; Wallace, G. G. A Single Component Conducting Polymer Hydrogel as a Scaffold for Tissue Engineering. Adv. Funct. Mater. 2012, 22, 2692-2699.
- (33) Guarino, V.; Alvarez-Perez, M. A.; Borriello, A.; Napolitano, T.; Ambrosio, L. Conductive PANi/PEGDA Macroporous Hydrogels for Nerve Regeneration. Adv. Healthcare Mater. 2013, 2, 218-227.

- (34) Ding, H.; Zhong, M.; Kim, Y. J.; Pholpabu, P.; Balasubramanian, A.; Hui, C. M.; He, H.; Yang, H.; Matyjaszewski, K.; Bettinger, C. J. Biologically Derived Soft Conducting Hydrogels Using Heparin-Doped Polymer Networks. ACS Nano 2014, 8, 4348–4357.
- (35) Wei, D.; Lin, X.; Li, L.; Shang, S.; Yuen, M. C.-W.; Yan, G.; Yu, X. Controlled Growth of Polypyrrole Hydrogels. *Soft Matter* **2013**, *9*, 2832–2836.
- (36) Mukhopadhyay, S.; Maitra, U. Chemistry and Biology of Bile Acids. Curr. Sci. 2004, 87, 1666–1683.
- (37) Terech, P.; Talmon, Y. Aqueous Suspensions of Steroid Nanotubules: Structural and Rheological Characterizations. *Langmuir* **2002**, *18*, 7240–7244.
- (38) Pal, A.; Basit, H.; Sen, S.; Aswal, V. K.; Bhattacharya, S. Structure and Properties of Two Component Hydrogels Comprising Lithocholic Acid and Organic Amines. *J. Mater. Chem.* **2009**, *19*, 4325–4334.
- (39) Zhang, X.; Zou, J.; Tamhane, K.; Kobzeff, F. F.; Fang, J. Y. Self-Assembly of pH-Switchable Spiral Tubes: Supramolecular Chemical Springs. *Small* **2010**, *6*, 217–220.
- (40) Tamhane, K.; Zhang, X.; Zou, J.; Fang, J. Y. Assembly and Disassembly of Tubular Spherulites. *Soft Matter* **2010**, *6*, 1224–1228.
- (41) Terech, P.; Velu, S. K. P.; Pernot, P.; Wiegart, L. Salt Effects in the Formation of Self-Assembled Lithocholate Helical Ribbons and Tubes. J. Phys. Chem. B 2012, 116, 11344–11355.
- (42) Wang, H.; Xu, W.; Song, S.; Feng, L.; Song, A.; Hao, J. Hydrogels Facilitated by Monovalent Cations and Their Use as Efficient Dye Adsorbents. *J. Phys. Chem. B* **2014**, *118*, 4693–4701.
- (43) Yui, H.; Guo, Y.; Koyama, K.; Sawada, T.; John, G.; Yang, B.; Masuda, M.; Shimizu, T. Local Environment and Property of Water inside the Hollow Cylinder of a Lipid Nanotube. *Langmuir* **2005**, *21*, 721–727.
- (44) Guo, L.; Chowdhury, P.; Fang, J. Y.; Gai, F. Heterogeneous and Anomalous Diffusion inside Lipid Tubules. *J. Phys. Chem. B* **2007**, 111, 14244–14249.
- (45) Lei, J.; Liang, W.; Martin, C. R. Infrared Investigations of Pristine Polypyrrole Is the Polymer Called Polypyrrole Really Poly(pyrrole-co-hydroxypyrrole)? *Synth. Met.* **1992**, *48*, 301–312.
- (46) Zhang, X.; Zhang, J.; Song, W.; Liu, Z. Controllable Synthesis of Conducting Polypyrrole Nanostructures. *J. Phys. Chem. B* **2006**, *110*, 1158–1165.
- (47) Qu, L.; Shi, G. Q.; Chen, F. E.; Zhang, J. Electrochemical Growth of Polypyrrole Microcontainers. *Macromolecules* **2003**, *36*, 1063–1067.
- (48) Moon, Y. B.; Cao, Y.; Smith, P.; Heeger, A. J. X-Ray Scattering from Crystalline Polyaniline. *Polym. Commun.* **1989**, *30*, 196–199.
- (49) Dai, T.; Lu, Y. Polypyrrole hydro-sponges built up from mesoscopic scales. J. Mater. Chem. 2007, 17, 4797–4802.
- (50) Yan, H.; Saiani, A.; Gough, J. E.; Miller, A. F. Thermoreversible Protein Hydrogel as Cell Scaffold. *Biomacromolecules* **2006**, *7*, 2776–2782.
- (51) Aleshin, A. N. Polymer Nanofibers and Nanotubes: Charge transport and device Applications. *Adv. Mater.* **2006**, *18*, 17–27.
- (52) Wang, C.; Yin, S.; Chen, S.; Xu, H.; Wang, Z.; Zhang, X. Controlled Self-assembly Manipulated by Charge-Transfer Interactions: From Tubes to Vesicles. *Angew. Chem., Int. Ed.* **2008**, 47, 9049–9052.